ACS OMEGA

http://pubs.acs.org/journal/acsodf

Article

Targeting Staphylococcal Cell–Wall Biosynthesis Protein FemX Through Steered Molecular Dynamics and Drug-Repurposing Approach

Shakilur Rahman, Subham Nath, Utpal Mohan, and Amit Kumar Das*

Cite This: *ACS Omega* 2023, 8, 29292–29301

Read Online

ACCESS | Metrics & More | Article Recommendations | Supporting Information

ABSTRACT: *Staphylococcus aureus*-mediated infection is a serious threat in this antimicrobial-resistant world. *S. aureus* has become a "superbug" by challenging conventional as well as modern treatment strategies. Nowadays, drug repurposing has become a new trend for the discovery of new drug molecules. This study focuses on evaluating FDA-approved drugs that can be repurposed against *S. aureus* infection. Steered molecular dynamics (SMD) has been performed for Lumacaftor and Olaparib against staphylococcal FemX to understand their binding to the active site. A time-dependent external force or rupture force has been applied to the ligands to calculate the force required to dislocate the ligand from the binding pocket. SMD analysis indicates that Lumacaftor has a high affinity for the substrate binding pocket in comparison to Olaparib. Umbrella sampling exhibits that Lumacaftor possesses a higher free energy barrier to displace it from the ligand-binding site. The bactericidal activity of Lumacaftor and Olaparib has been tested, and it shows that Lumacaftor has moderate activity along with biofilm inhibition potential (MIC value with conc. 128 μg/mL). Pharmacokinetic and toxicology evaluations indicate that Lumacaftor has higher pharmacokinetic potential with lower toxicity. This is the first experimental report where staphylococcal FemX has been targeted for the discovery of new drugs. It is suggested that Lumacaftor may be a potential lead molecule against *S. aureus*.

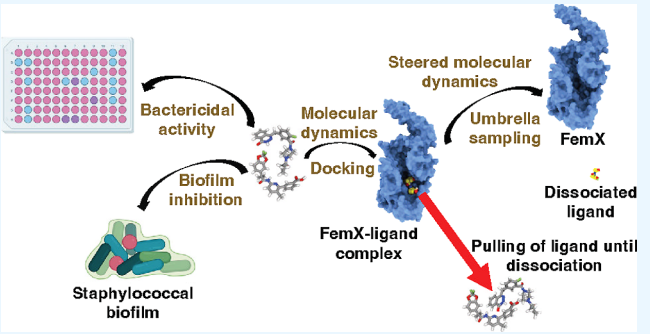

1. INTRODUCTION

The increasing prevalence of methicillin-resistant *Staphylococcus aureus* infections has gained attention in design and development of novel antibacterial agents.[1] *S. aureus* is one of the deadly microorganisms from the ESKAPE family of pathogens.[2] The resistance strategy of *S. aureus* to methicillin and other β-lactam antibiotics is generated by expressing a foreign penicillin-binding protein (PBP) known as PBP2a.[3] PBP2a can perform the functions of host PBPs and bypass the action of β-lactam antibiotics. Additionally, several other auxillary (aux) genes have also been identified that play a crucial role in methicillin resistance, namely, factors essential for methicillin-resistance (fem) family genes.[4] Three of these genes, *femX*, *femA*, and *femB*, play a vital role in the latter stage of the peptidoglycan (PG) biosynthesis process of *Staphylococci* and can be served as potential targets for developing new antimicrobial therapeutics.[5,6] Staphylococcal PG-repeat unit consists of a disaccharide, a pentapeptide stem, and a penta-glycine bridge structure. The PG disaccharide unit (DU) is composed of *N*-acetyl-glucosamine (NAG) and *N*-acetyl-muramic acid (NAM) and is conserved among all eubacteria, whereas the pentapeptide stem and bridge structure vary between species.[7] FemX, FemA, and FemB add five glycine residues to the lysine of the A-E-K-A-A pentapeptide stem, thereby developing the flanking bridge structure. FemX adds the first glycine, FemA adds the second and third glycine, and FemB adds the fourth and fifth glycine to the lysine of the pentapeptide stem.[8]

This pentaglycine (Gly_5) bridge is essential for crosslinking several PG chains to develop a 20–40 nm thick cell wall.[9,10] The C-terminal of the Gly_5 bridge forms an amide bond to the side chain nitrogen of the L-lysine of the A-E-K-A-A pentapeptide stem.[11] During the final stage of PG synthesis, a mature cell wall was developed by crosslinking the N-terminal of a pentaglycine bridge structure to the D-Ala (4th amino acid of a pentapeptide stem) of a neighboring PG chain with a peptide bond (Figure 1).[12] This crosslinking provides the Gram-positive characteristic mesh-like PG structure to the cell wall. All these fem family enzymatic reactions are highly substrate-specific, where mutations or deletions of the genes can lead to decreased resistance to β-lactam compounds and

Received: April 19, 2023
Accepted: July 24, 2023
Published: August 2, 2023

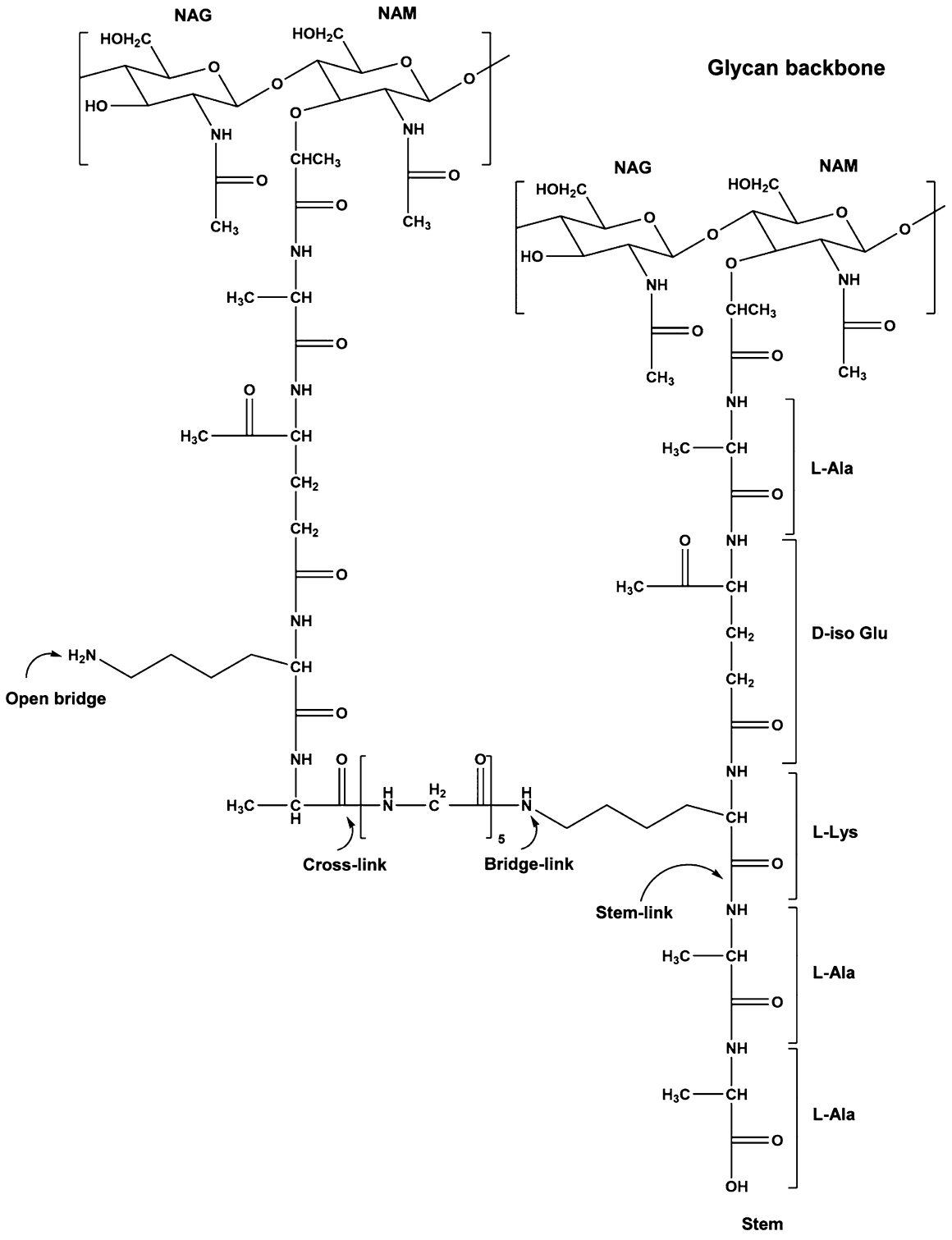

Figure 1. Chemical composition of *S. aureus* PG. The DU comprises NAG and NAM. The pentapeptide structure is formed with L-Ala−D-Glu−L-Lys−-Ala−D-Ala, where the glycine bridge is attached to the ε nitrogen of L-Lys of the third position of the pentapeptide stem. Crosslinking occurs between the N-terminus of the last glycine of the bridge with the D-Ala (fourth position) of the adjacent pentapeptide stem.

PG crosslinking.[13−15] More importantly, the deletion of *femX* in *S. aureus* is lethal,[14,16] whereas the deletion of *femA* and *femB* results in the synthesis of mono and tri-glycyl segments in bridge structure (Figure 2).[8,17]

In contrast to Gram-negative bacteria, which have an outer membrane, Gram-positive bacteria have layers of PG that are many times thicker than Gram-negative bacteria. Over the past few decades, the PG biosynthesis pathway has been the most attractive target for designing novel antibiotics. PBPs were the primary targets for many years, but due to the accumulation of foreign PBP, treating *S. aureus* has become a severe issue. This has led us to search for new drug molecules against drug-resistant *S. aureus*. The current study presents steered molecular dynamics (SMDs) and umbrella sampling (US)

https://doi.org/10.1021/acsomega.3c02691
ACS Omega 2023, 8, 29292−29301

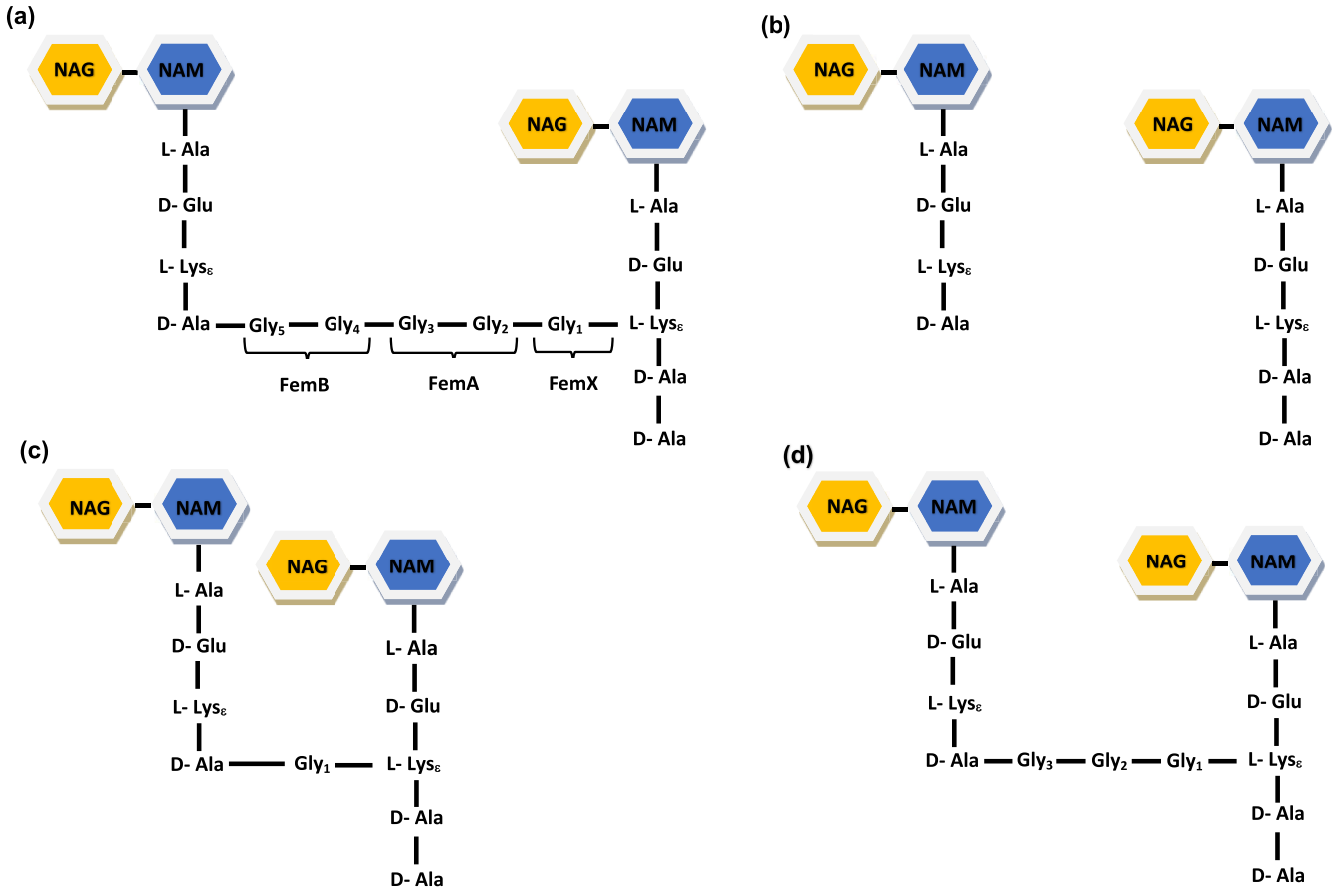

Figure 2. Structure of *S. aureus* PG consists of disaccharide, pentapeptide stem (L-Ala−D-Glu−L-Lys−D-Ala−D-Ala), and glycine bridge structure. (a) Proper crosslinking of PG chain where no mutation/deletion is present either in staphylococcal FemX, FemA, or FemB, (b) no crosslinking of PG chain due to mutation/deletion in FemX, (c) very short crosslinking of PG chain due to mutation/deletion in FemA, and (d) short crosslinking of PG chain due to mutation/deletion in FemB.

analysis of the FemX-drug complexes, the bactericidal activity of the selected drugs, biofilm inhibition assay, and ADMET evaluation of the selected drugs.

2. MATERIALS AND METHODS

2.1. Steered Dynamics and US. Pulling simulations are essential to estimate the binding energy between Lumacaftor and staphylococcal FemX. The Lumacaftor-FemX and Olaparib−FemX complex structures were obtained from our previous Study.[18] Protein topology was generated with AMBER99SB forcefield, and ligand topology was generated using the general AMBER force field[19] from the ACPYPE server.[20] The pulling direction was determined based on the drug-binding pocket of FemX, where the drug-binding pocket was made parallel to the *Z*-axis. FemX-drug complexes were positioned in a rectangular box with dimensions sufficient to provide a place for pulling simulations to be performed along the *Z*-axis. The simulation system was solvated using TIP3P water, and counter ions were added to neutralize the net charge of the system. Long-range electrostatic interactions were treated using the particle mesh Ewald method, and a steepest-descent minimization of 50,000 steps was used the remove the bad contacts from the system. The system was equilibrated in an *NVT* ensemble at 1 atm pressure and 310 K temperature with the Berendsen thermostat. For each system, the FemX backbone was kept constrained, whereas drugs were pulled from the protein active site toward the solvent pull along the *Z*-axis. Both the ligands were pulled at 0.01 nm/ps by using a spring constant of 1000 kJ mol^{-1} nm^{-2}. The final steered molecular dynamics (SMD) simulation of 1000 ps was performed with Berendsen temperature coupling and Parrinello−Rahman pressure coupling using the GROMACS 2020.0 package.[21] Single pulling vector and exit trajectory were explored during SMD. The snapshots so obtained from SMD trajectories were exploited for umbrella sampling (US). During sampling, window spacing was kept at 0.1 nm for the center of mass separation. The system was further subjected to NPT equilibration for 100 ps. During US, a 10 ns simulation was performed for each selected individual configuration. The weighted histogram analysis method module was used to calculate the potential mean force (PMF) from the outcomes of the US simulations.

2.2. Bacterial Strains, Culture Conditions, and Chemical Stocks. *S. aureus* MTCC 3160 and NCTC 8325 strains (both are methicillin-sensitive; MSSA) were used in this study. A single colony of *S. aureus* was cultured overnight in 5 mL Mueller Hinton broth (MH; HiMedia, India) at 37 °C with 150 rpm agitation. To prepare the stock solution, Lumacaftor and Olaparib (Selleck Chemicals, USA) were dissolved in dimethyl sulfoxide or DMSO (Sigma-Aldrich Inc., USA) to the final concentration of 1 mg/mL and stored at −20 °C for further use.

2.3. Bactericidal Activity Assay. Minimum inhibitory concentrations of drugs were calculated based on a previously

https://doi.org/10.1021/acsomega.3c02691
ACS Omega 2023, 8, 29292−29301

described broth microdilution method.[22] 100 μL of Lumacaftor (512 μg/mL) and Olaparib (512 μg/mL) were added individually to the first column of a 96 well-plate (Thermo Fisher Scientific, USA), and two-fold serial dilutions of drugs were added to the other wells. Then, 50 μL of bacterial suspension (10^6 CFU/mL) was seeded to each well for a final concentration of 10^5 CFU/mL. Amp-Na (6.25 μg/mL) was used as the positive control. The plate was kept in an incubator at 37 °C for 16 h. The optical density (OD) of bacterial cultures was measured at 600 nm using a plate reader (BioTek, USA). Each sampling was done in triplicate for quantification. Data are presented as mean standard deviation. Statistical comparisons between groups were performed by Student's *t*-test. $P < 0.05$ was considered to be statistically significant.

2.4. Biofilm Inhibition Assay. A 96-well microtiter plate was prepared according to the method described above. The plate was incubated at 37 °C for 16 h under static conditions. *Trans*-Chalcone (20 μg/mL) was used as a positive control.[23,24] After incubation, non-adherent cells were removed, and the wells were washed twice using PBS. The plate was dried for 15 min in laminar airflow, and the biofilm was stained with filtered 0.1% (w/v) crystal violet (CV) for 20 min at room temperature. The excess stain was removed by washing with PBS three times. Then, 95% ethanol was added to the wells and incubated for 10 min. Absorption of the CV stain was recorded at 570 nm using a micro-titer plate reader (BioTek, USA). Each sampling was done in a triplicate manner. Statistical comparisons between groups were performed by Student's *t*-test, where $p < 0.05$ was considered to be statistically significant.

2.5. ADME and Toxicity Evaluation. To evaluate the physicochemical properties and toxicity of the drug, the two-dimensional (2D) structure and SMILES of Lumacaftor (PubChem CID: 16678941) and Olaparib (PubChem CID: 23725625) were obtained from the PubChem database.[25] SwissADME[26] was used to calculate the molecular weight, lipophilicity, polarity, insolubility, flexibility, insaturation, GI absorption, and blood−brain barrier (BBB) permeation. Further, toxicity properties, such as maximum tolerance dose, cytochrome P450 (CYP) inhibitory activity, skin sensitization, and so forth, were predicted using the pkCSM tool.[27]

3. RESULTS

3.1. Steered Dynamics and US. The interaction energy between Lumacaftor and staphylococcal FemX was calculated to understand the strength of the interaction of drug and protein. In steered MD simulations, a time-dependent external force is applied on the ligands to drive its dislocation from the protein, which cannot usually be achieved by standard MD simulation. Notably, the transition between the bound and unbound states has been measured during steered MD. The force was gradually increased concerning time (ps) and distance (nm). Lumacaftor had a steady increase in the applied force until the force reached the maximum value of 3501.17 kJ/mol/nm at around 450 ps time, termed rupture force (F_{max}). In contrast, Olaparib had a significantly lower F_{max} of 1471.71 kJ/mol/nm at around 200 ps time (Figure 3). The force then rapidly decreased and remained constant until the end of the simulation, suggesting the disruption in ligand−receptor interactions. SMD shows that both drugs attain different F_{max} at different time points. Reaction coordinates achieved from SMD were further used for US. US allowed us to calculate the potential mean force (PMF) required to separate the ligand from FemX. The snapshots which were obtained from SMD trajectories were exploited for US. The PMF result showed that Lumacaftor required more energy than Olaparib to dislocate it from the ligand-binding site (Figure 4). Lumacaftor exhibited a higher free energy barrier at approximately 87.41 kJ/mol compared to Olaparib, which possessed a PMF of 32.31 kJ/mol. These results from US completely resonate with the SMD study. These drugs were used for further experimental investigation.

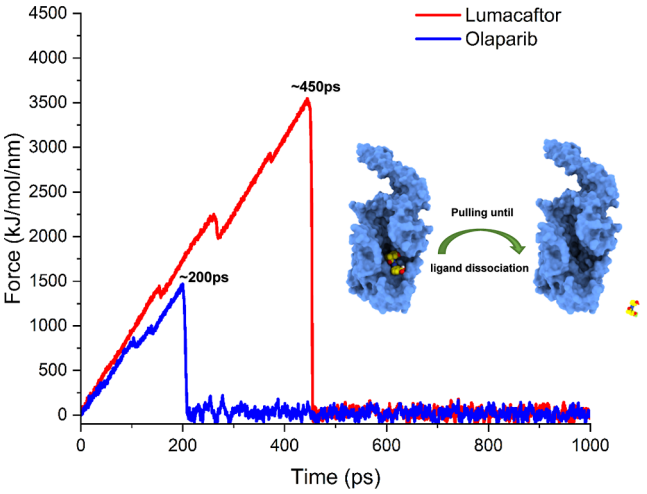

Figure 3. SMD simulation of Lumacaftor and Olaparib showing the rupture force profile. The *x*-axis denotes the simulation time, whereas the *y*-axis denotes the pulling-out force required to dislocate the ligands from their respective binding sites.

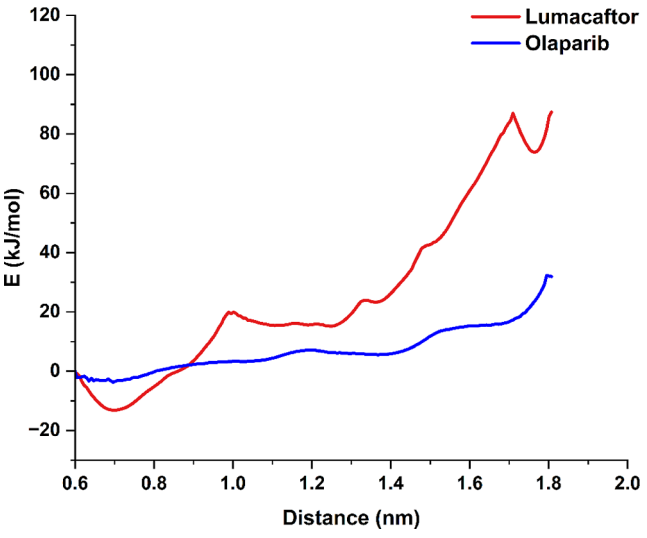

Figure 4. Potential mean force (PMF) curves of Lumacaftor and Olaparib complexes obtained from US.

3.2. Minimum Inhibitory Concentration and IC_{50}. Minimum inhibitory concentration was determined to assess the antibacterial activity of Lumacaftor and Olaparib against Gram-positive *S.aureus*. Lumacaftor displayed antibacterial activity at an inhibitory concentration of 128 μg/mL for both the *S. aureus* strains (Figure 5). In contrast, Olaparib did not exhibit any notable antibacterial activity against *S. aureus* at any concentration tested (Figure S1). The MIC value for Lumacaftor was determined with conc. 128 μg/mL, and the

https://doi.org/10.1021/acsomega.3c02691
ACS Omega 2023, 8, 29292−29301

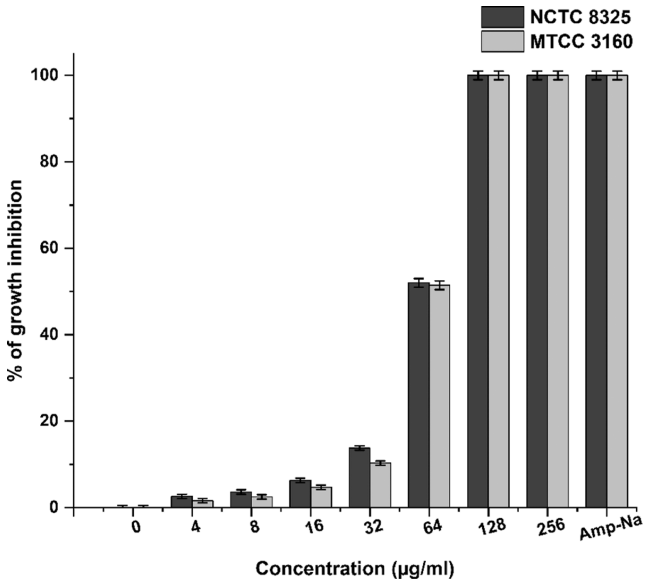

Figure 5. Bactericidal activity of Lumacaftor by the microdilution method in terms of minimum inhibitory concentration (MIC). The MIC value for Lumacaftor was determined with a concentration of 128 μg/mL and IC_{50} value with a ∼65 μg/mL concentration for *S. aureus* NCTC 8325 and MTCC 3160 strains. Statistical comparisons were performed using Student's *t*-test, where $P < 0.05$ was considered to be statistically significant.

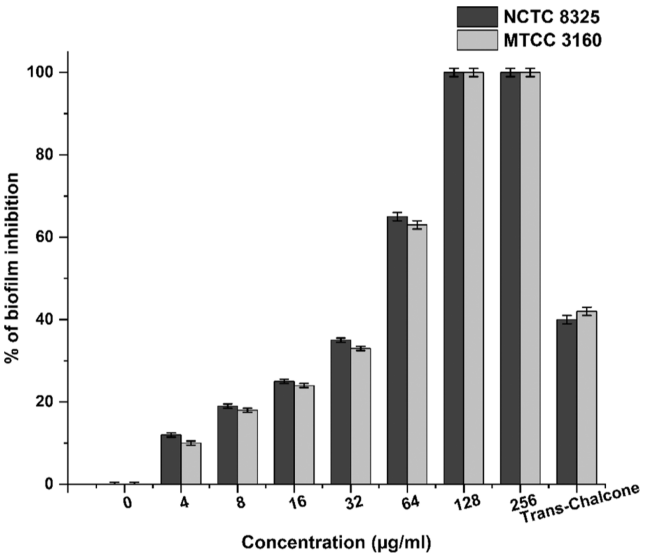

Figure 6. Susceptibility of *Staphylococcus aureus* biofilms to inhibition by Lumacaftor. The percentage of biofilm inhibition after treatment with Lumacaftor indicates the efficacy of the drug against *S. aureus* NCTC 8325 and MTCC 3160 strains. Statistical comparisons were performed using Student's *t*-test, where $P < 0.05$ was considered to be statistically significant.

IC_{50} value was determined with conc. ∼65 μg/mL. These data suggested that Lumacaftor has moderate inhibitory activity against *S. aureus* NCTC 8325 and MTCC 3160 and it could be a promising lead compound for developing new treatments against planktonic *S. aureus*. Overall, these findings demonstrate the potential of Lumacaftor as a candidate for further exploration in the field of antibacterial drug discovery.

3.3. Biofilm Inhibition. The CV assay was performed to evaluate the effect of Lumacaftor and Olaparib on biofilm biomass. The results showed that Lumacaftor had a moderate impact on biofilm biomass at sub-inhibitory concentrations and a high impact on biofilm growth at the minimum inhibitory concentration after 16 h of treatment. At sub-inhibitory concentrations, Lumacaftor was able to reduce biofilm biomass by 10−60%, while the positive control *trans*-Chalcone was only able to achieve a ∼40% reduction (Figure 6). These data indicated the potential of Lumacaftor to inhibit staphylococcal biofilm growth. On the other hand, Olaparib did not show any biofilm inhibition activity (Figure S2). The CV assay results provided valuable insights into the potential of Lumacaftor in inhibiting biofilm growth, which can have important implications for the development of new therapies for *S.aureus*-mediated infections. Besides, assays showed that both the drugs are found to be ineffective to eradicate staphylococcal biofilms; results are shown in Tables S1 and Table S2.

4. ADMET

An *in silico* ADME study analyzed the physicochemical properties, lipophilicity, water solubility pharmacokinetics, drug-likeness, and medicinal chemistry properties of Lumacaftor and Olaparib. SwissADME showed that Lumacaftor and Olaparib were not violating any of the Lipinski rules of five. They were found to follow the Ghose, Veber, Egan, and Muegge rules with a good bioavailability score of 0.56 and 0.55 for Lumacaftor and Olaparib, respectively. The bioavailability radar (Spider plot) of Lumacaftor showed that all the 6 parameters, such as lipophilicity (XLOGP3 = 4.40), size (MV = 434.46 g/mol), polarity (TPSA = 97.75 A^2), insolubility (LOG S{ESOL} = −5.45), and flexibility (number of rotatable bonds = 6) lie within the acceptable range except insaturation (Fraction C sp^3 = 0.21; where range lies between 0.25 and 1.00), which was found to be just outside the acceptable range (Table 1) (Figure 7). Besides, the spider plot of Olaparib

Table 1. Pharmacokinetic Evaluation of Lumacaftor Using SwissADME

parameters	properties	
	Lumacaftor	Olaparib
molecular weight	452.41 g/mol	434.46
lipophilicity	4.40	1.90
polarity	97.75 A^2	86.37 A^2
insolubility	−5.45	−3.70
flexibility in terms of the number of rotatable bonds	6	6
insaturation	0.21	0.33
GI absorption	high	high
BBB permeant	no	no
log K_p (Skin permeation)	−5.91 cm/s	−7.60 cm/s

exhibited that all these parameters, such as lipophilicity (XLOGP3 = 1.90), size (MV = 452.41 g/mol), polarity (TPSA = 86.37 A^2), insolubility (LOG S{ESOL} = −3.70), flexibility (number of rotatable bonds = 6), and insaturation (Fraction C sp^3 = 0.33) lie within the acceptable range. ADME analysis depicted that both Lumacaftor and Olaparib have high gastrointestinal (GI) absorption (78.71 and 91.92%, respectively) and skin permeability. The BOILED-Egg model of Lumacaftor and Olaparib lies in the white region, suggesting that the two compounds are highly likely to be absorbed by the gastrointestinal tract (Figure 7). Importantly, neither drug was

https://doi.org/10.1021/acsomega.3c02691
ACS Omega 2023, 8, 29292−29301

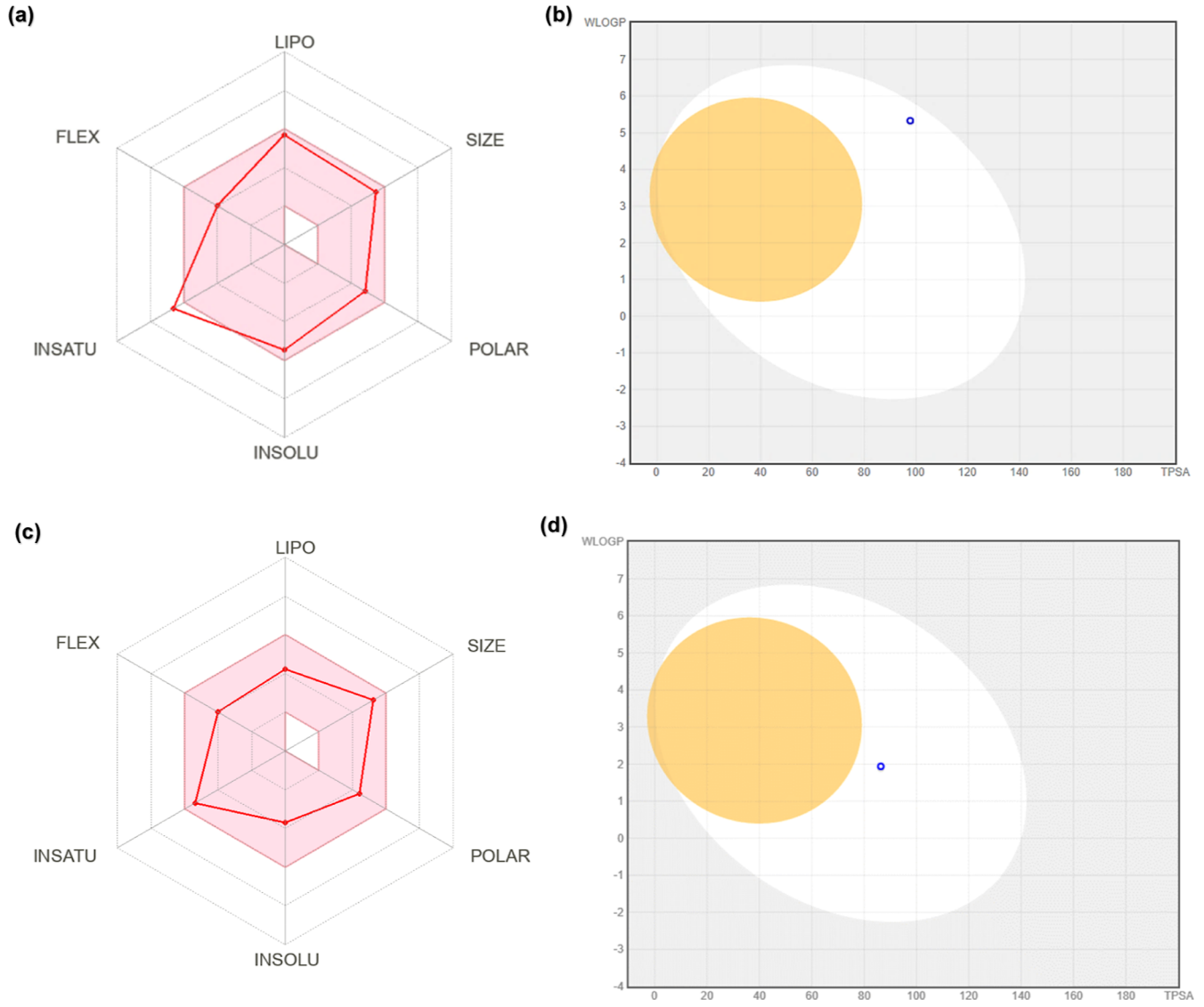

Figure 7. Bioavailability radar and BOILED-egg models of Lumacaftor and Olaparib based on physicochemical descriptors. The pink zone in the bioavailability radar is the ideal physicochemical space for oral bioavailability in the case of Lumacaftor (a) and Olaparib (c). BOILED-egg models predicted the GI absorption and BBB permeation of Lumacaftor (b) and Olaparib (d).

crossing the BBB, which is considered an important property to consider these drugs for usage. The pkCSM tool provided several other pieces of information about the toxicity of the drugs (Table 2). Lumacaftor and Olaparib exhibited a maximum tolerated dose of 0.824 log mg/kg/day and 0.204 (log mg/kg/day) for humans. Besides, Lumacaftor showed oral acute toxicity (LD_{50}) of 2.797 (mol/kg) and oral chronic toxicity (LOAEL) of 1.424 (log mg/kg_bw/day). Olaparib showed oral acute toxicity (LD_{50}) of 2.623 (mol/kg) and oral chronic toxicity (LOAEL) of 1.799 (log mg/kg_bw/day). Both drugs have no skin sensitization effect. Lumacaftor was not an inhibitor for CYP1A2, CYP2C19, CYP2D6, or CYP3A4 except CYP2C9, and Olaparib was found to be a CYP2C19 and CYP2C9 inhibitor. There were fewer chances of unwanted adverse effects due to the lower clearance and accumulation of these drugs.

5. DISCUSSION

Drug development is a time-consuming, costly, and challenging process with a high degree of uncertainty that a drug will actually become effective. Here, drug repurposing comes into play, which involves exploring new therapeutic usage of existing approved, discontinued, shelved, and investigational drugs. Drug repurposing is a novel way of finding new uses outside the scope and offers reduced cost and faster development timeline and regulatory approval, as these drugs already have positive preclinical and safety data. This study focuses on eliminating *S. aureus* with existing market-available drugs.

Our previous work engaging virtual screening, docking, conventional molecular dynamics (CMD), and hybrid quantum mechanics/molecular mechanics (QM/MM) studies reported that Lumacaftor and Olaparib could be used as repurposing drugs against staphylococcal FemX.[18] The docking study showed that Lumacaftor has a higher affinity in terms of K_d value than Olaparib. Besides, the molecular dynamics study reported that the FemX−Lumacaftor complex is more stable than the FemX−Olaparib complex. Further, molecular mechanics/generalized-born surface area (MM/GBSA) calculations also indicated that Lumacaftor has higher

https://doi.org/10.1021/acsomega.3c02691
ACS Omega 2023, 8, 29292−29301

Table 2. Toxicology Evaluation of Lumacaftor Using pkCSM

parameters	properties	
	Lumacaftor	Olaparib
intestinal absorption (human)	78.71%	91.92%
CYP1A2 inhibitor	no	no
CYP2C19 inhibitor	no	yes
CYP2C9 inhibitor	yes	yes
CYP2D6 inhibitor	no	no
CYP3A4 inhibitor	no	yes
renal OCT2 substrate	no	no
maximum tolerated dose (human)	0.824 (log mg/kg/day)	0.204 (log mg/kg/day)
hERG I inhibitor	no	no
hERG II inhibitor	no	yes
oral rat acute toxicity (LD_{50})	2.797 (mol/kg)	2.623 (mol/kg)
oral rat chronic toxicity (LOAEL)	1.424 (log mg/kg_bw /day)	1.799 (log mg/kg_bw /day)
skin sensitization	no	no

binding energies toward FemX in comparison with Olaparib. SMDs is a modern method to study the ligand−receptor unbinding mechanisms.[28,29] This study uses SMD and US to estimate the pulling force and PMF required to dislocate the drugs from their ligand-binding sites in FemX. Lumacaftor possesses a higher pulling force and PMF than Olaparib when ligands are pulled with a time-dependent external force (Figures 3 and 4). The reason behind this significant variation in F_{max} peaks for the selected hits is due to the different interaction profiles of the drugs with FemX. Previous *in silico* and *in vitro* studies also reported that drugs possess the same dissociation trend during SMD and US.[28−33] Lumacaftor and Olaparib possess two and three H-bonds with FemX, respectively. Interaction between Lumacaftor and FemX is mainly stabilized by strong $\pi-\pi$ interactions between aromatic residues of receptor and aromatic rings of ligands.[18] SMD and US data support the findings from conventional molecular dynamics and hybrid QM/MM studies, which in turn offer the acceptability of the current study.

The PG layer maintains the cell-membrane integrity and is essential for bacterial survival. The PG biosynthesis pathway is the most widely targeted area for designing new and potent antibiotics.[34,35] Comprehensive information on the mechanism of methicillin resistance paved the way for discovering auxiliary factors such as Fem, which regulates the methicillin resistance in *S. aureus*. FemXAB activity is highly substrate-specific, where FemX mutations/deletion is lethal to *S. aureus*.[16] Ampicillin-sodium (Amp-Na), which is used in this study as a positive control, is a member of the extended-spectrum β-lactam family. Nowadays, resistance to β-lactams in *S.aureus*-mediated infections is a serious healthcare concern.[36] The prevalence of antibiotic resistance among pathogens is a growing problem that draws attention to the development of new antibiotics.[37] However, β-lactam antibiotics cause medication error that has been recognized as a common and serious threat to patient safety.[38] β-Lactam antibiotics are found to be involved with severe adverse effects.[39,40] Thereby, new drugs are being explored against *S. aureus* using a drug-repurposing approach.[41−43] Our study showed that Lumacaftor has decent bactericidal activity (MIC: 128 μg/mL), but Olaparib had no potential against *S. aureus* MTCC 3160 and NCTC 8325 strains (Figure 5). Surprisingly, we have found that Lumacaftor can inhibit biofilm formation by 10−60% with the sub-inhibitory concentrations, which indicates its potential as an anti-biofilm agent. Previous studies also showed that drugs could significantly inhibit biofilm formation at sub-inhibitory concentrations.[44,45] CMD and SMD studies also indicated that Lumacaftor might have more potential against *S. aureus*. Lumacaftor was significantly able to inhibit staphylococcal biofilm formation (Figure 6). Previous studies reported that FDA-approved drugs with higher F_{max} values possess higher biological activity.[46,47] These previous reports evaluate the robustness of our currently employed approach. Based on the literature, no such standard drug is available against staphylococcal FemX, so we could not perform any comparison. Combination antibiotic treatment against bacterial infections is an attractive alternative as it could address the shortcomings of most antibiotics. Recently, antibiotic combinations have been used against *S. aureus* and other bacteria to increase the efficiency and reduce the resistance to any individual drugs.[48−51] Thereby, we suggest that the synergistic use of Lumacaftor with other antibiotics can increase drug activity and bacterial elimination.

Many medications have failed during the drug development process due to poor pharmacokinetics and toxicity issues.[52] Problems that arise during the drug development process could be resolved early on. *In silico* ADMET methods are the first step in this pipeline process to assess the issues of new chemical compounds.[53] ADMET factors reveal how chemical substances behave within a living being. These techniques save time by avoiding lead candidates that would be harmful or would be converted by the body into an inactive form. These ADMET parameters disclose the behavior of the chemical compounds in a living organism. In this study, Lumacaftor and Olaparib were evaluated for their pharmacokinetic potential. SwissADME and pkCSM use a combination of *in silico* models and experimental data to make their predictions using the input of accurate and complete molecular information such as 2D/3D structure, charges, and tautomeric forms.[26,27] The BOILED-egg model predicts the gastrointestinal absorption and BBB permeation of the given drug.[54] Both drugs show high GI absorption values with no BBB permeation potential, indicating their acceptability as promising therapeutic agents (Figure 7). The Lipinski filter is the pioneer rule of five, and none of the drugs is found to violate any of the rules. Besides, the CYP superfamily of isoenzymes is crucial in drug elimination through metabolic pathways. Inhibition of five major CYP isoenzymes such as CYP1A2, CYP2C19, CYP2CP, CYP2D6, and CYP3A4 is certainly one major cause of pharmacokinetics-related drug−drug interactions that may lead to toxic effects due to accumulation and lower clearance of the drug.[55−57] Lumacaftor was found to be a CYP2C9 inhibitor, whereas Olaparib was found to be a CYP2C19 and CYP2C9 inhibitor (Table 2). These data indicated that Lumacaftor could be less toxic than Olaparib. Moreover, these are FDA-approved drugs, which means they have already been validated for therapeutic use, outweighing the intended usage risks. Importantly, none of the drugs may elicit any allergic response in susceptible individuals due to a lack of skin sensitization effect. The collective data suggest that Lumacaftor may be considered as a lead molecule or a prototype for developing new derivatives.

https://doi.org/10.1021/acsomega.3c02691
ACS Omega 2023, 8, 29292−29301

6. CONCLUSIONS

This study evaluates the activity of two drugs, Lumacaftor and Olaparib, against *S. aureus*. The study targets *S. aureus* FemX—the protein involved in building the bacterial cell wall. *In silico* analysis shows that Lumacaftor requires significantly more energy (PMF) than Olaparib to be dislodged from the binding site of FemX. Lumacaftor has moderate bactericidal activity with a MIC value of 128 μg/mL and inhibits the planktonic growth of the *S. aureus* MTCC3160 and NCTC 8325 strains. On the other hand, Olaparib does not show any bactericidal activity. Moreover, Lumacaftor inhibits biofilm formation even when treated with sub-inhibitory concentration, but Olaparib does not inhibit it. It may be concluded that Lumacaftor can be a potential lead molecule against *S. aureus* for further development as an antibiotic.

■ ASSOCIATED CONTENT

Supporting Information

The Supporting Information is available free of charge at https://pubs.acs.org/doi/10.1021/acsomega.3c02691.

Bactericidal and biofilm inhibition activity of Olaparib against *S. aureus* strains and biofilm eradication activity by Lumacaftor and Olaparib against *S. aureus* strains and (PDF)

SMD trajectories where Lumacaftor and Olaparib were pulled out of the active site of FemX (ZIP)

■ AUTHOR INFORMATION

Corresponding Author

Amit Kumar Das − *Department of Biotechnology, Indian Institute of Technology Kharagpur, Kharagpur, West Bengal 721302, India;* orcid.org/0000-0001-9703-1898; Phone: +91-3222-283756; Email: amitk@bt.iitkgp.ac.in

Authors

Shakilur Rahman − *Department of Biotechnology, Indian Institute of Technology Kharagpur, Kharagpur, West Bengal 721302, India;* orcid.org/0000-0001-5180-3581

Subham Nath − *National Institute of Pharmaceutical Education and Research Kolkata, Kolkata, West Bengal 700054, India*

Utpal Mohan − *National Institute of Pharmaceutical Education and Research Kolkata, Kolkata, West Bengal 700054, India;* orcid.org/0000-0002-0256-7305

Complete contact information is available at: https://pubs.acs.org/10.1021/acsomega.3c02691

Author Contributions

S.R. conceptualized the study, performed SMD simulation, and US experiments and wrote the draft manuscript. S.N. performed MIC and biofilm inhibition studies. U.M. and A.K.D. supervised the work and improvised the final manuscript.

Notes

The authors declare no competing financial interest.

GROMACS 2020.0 is an open-source package freely available from the source (http://ftp.gromacs.org/pub/gromacs/gromacs-2020.tar.gz). Protein structure is available in Protein Data Bank (PDB ID: 6SNR). Ligand information is publicly available in the PubChem database (https://pubchem.ncbi.nlm.nih.gov/).

■ ACKNOWLEDGMENTS

This work has been carried out with financial assistance from the Science and Engineering Research Board, Government of India (GOI), file no. CRG/2020/002622. S.R. acknowledges the Indian Institute of Technology Kharagpur for individual fellowship. The authors would like to acknowledge Ranabir Majumder, Maniklal Shee, and Rituparna Saha, IIT Kharagpur, for critical suggestions. This work used the computational resources of the PARAM shakti supercomputing facility of IIT Kharagpur (www.hpc.iitkgp.ac.in), established under the National Supercomputing Mission of the Government of India (GoI) and supported by CDAC, Pune.

■ REFERENCES

(1) Benson, T. E.; Prince, D. B.; Mutchler, V. T.; Curry, K. A.; Ho, A. M.; Sarver, R. W.; Hagadorn, J. C.; Choi, G. H.; Garlick, R. L. X-Ray Crystal Structure of Staphylococcus Aureus FemA. *Structure* **2002**, *10*, 1107−1115.

(2) Santajit, S.; Indrawattana, N. Mechanisms of Antimicrobial Resistance in ESKAPE Pathogens. *BioMed Res. Int.* **2016**, *2016*, 1−8.

(3) Lim, D.; Strynadka, N. C. J. Structural Basis for the β Lactam Resistance of PBP2a from Methicillin-Resistant Staphylococcus Aureus. *Nat. Struct. Biol.* **2002**, *9*, 870−876.

(4) Berger-Bächi, B.; Tschierske, M. Role of Fem Factors in Methicillin Resistance. *Drug Resist. Updates* **1998**, *1*, 325−335.

(5) Monteiro, J. M.; Covas, G.; Rausch, D.; Filipe, S. R.; Schneider, T.; Sahl, H.-G.; Pinho, M. G. The Pentaglycine Bridges of Staphylococcus Aureus Peptidoglycan Are Essential for Cell Integrity. *Sci. Rep.* **2019**, *9*, 5010.

(6) Rahman, S.; Das, A. K. Integrated Multi-Omics, Virtual Screening and Molecular Docking Analysis of Methicillin-Resistant Staphylococcus Aureus USA300 for the Identification of Potential Therapeutic Targets: An In-Silico Approach. *Int. J. Pept. Res. Ther.* **2021**, *27*, 2735−2755.

(7) Kim, S. J.; Chang, J.; Singh, M. Peptidoglycan Architecture of Gram-Positive Bacteria by Solid-State NMR. *Biochim. Biophys. Acta Biomembr.* **2015**, *1848*, 350−362.

(8) Rohrer, S.; Berger-Bächi, B. FemABX Peptidyl Transferases: A Link between Branched-Chain Cell Wall Peptide Formation and β-Lactam Resistance in Gram-Positive Cocci. *Antimicrob. Agents Chemother.* **2003**, *47*, 837−846.

(9) Gally, D.; Archibald, A. R. Cell Wall Assembly in Staphylococcus Aureus: Proposed Absence of Secondary Crosslinking Reactions. *J. Gen. Microbiol.* **1993**, *139*, 1907−1913.

(10) Giesbrecht, P.; Kersten, T.; Maidhof, H.; Wecke, J. Staphylococcal Cell Wall: Morphogenesis and Fatal Variations in the Presence of Penicillin. *Microbiol. Mol. Biol. Rev.* **1998**, *62*, 1371−1414.

(11) Tong, G.; Pan, Y.; Dong, H.; Pryor, R.; Wilson, G. E.; Schaefer, J. Structure and Dynamics of Pentaglycyl Bridges in the Cell Walls of Staphylococcus Aureus by 13 C− 15 N REDOR NMR. *Biochemistry* **1997**, *36*, 9859−9866.

(12) Vollmer, W.; Blanot, D.; de Pedro, M. A. Peptidoglycan Structure and Architecture. *FEMS Microbiol. Rev.* **2008**, *32*, 149−167.

(13) Strandén, A. M.; Ehlert, K.; Labischinski, H.; Berger-Bächi, B. Cell Wall Monoglycine Cross-Bridges and Methicillin Hypersusceptibility in a FemAB Null Mutant of Methicillin-Resistant Staphylococcus Aureus. *J. Bacteriol.* **1997**, *179*, 9−16.

(14) Rohrer, S.; Ehlert, K.; Tschierske, M.; Labischinski, H.; Berger-Bächi, B. The Essential Staphylococcus Aureus Gene FmhB Is Involved in the First Step of Peptidoglycan Pentaglycine Interpeptide Formation. *Proc. Natl. Acad. Sci. U.S.A.* **1999**, *96*, 9351−9356.

(15) Sharif, S.; Kim, S. J.; Labischinski, H.; Schaefer, J. Characterization of Peptidoglycan in Fem -Deletion Mutants of Methicillin-Resistant Staphylococcus Aureus by Solid-State NMR. *Biochemistry* **2009**, *48*, 3100−3108.

(16) Tschierske, M.; Mori, C.; Rohrer, S.; Ehlert, K.; Shaw, K. J.; Berger-Bächi, B. Identification of Three Additional FemAB -like Open

Reading Frames in Staphylococcus Aureus. *FEMS Microbiol. Lett.* **1999**, *171*, 97−102.
(17) Labischinski, H. The Targeting of Factors Necessary for Expression of Methicillin Resistance in Staphylococci. *J. Antimicrob. Chemother.* **1998**, *41*, 581−584.
(18) Rahman, S.; Rajak, K.; Mishra, S.; Das, A. K. Identification of Potential Inhibitors against FemX of Staphylococcus Aureus: A Hierarchial in-Silico Drug Repurposing Approach. *J. Mol. Graph. Model.* **2022**, *115*, 108215.
(19) Wang, J.; Wolf, R. M.; Caldwell, J. W.; Kollman, P. A.; Case, D. A. Development and Testing of a General Amber Force Field. *J. Comput. Chem.* **2004**, *25*, 1157−1174.
(20) Sousa da Silva, A. W.; Vranken, W. F. ACPYPE - AnteChamber PYthon Parser InterfacE. *BMC Res. Notes* **2012**, *5*, 367.
(21) Abraham, M. J.; Murtola, T.; Schulz, R.; Páll, S.; Smith, J. C.; Hess, B.; Lindahl, E. GROMACS: High Performance Molecular Simulations through Multi-Level Parallelism from Laptops to Supercomputers. *SoftwareX* **2015**, *1−2*, 19−25.
(22) Wiegand, I.; Hilpert, K.; Hancock, R. E. W. Agar and Broth Dilution Methods to Determine the Minimal Inhibitory Concentration (MIC) of Antimicrobial Substances. *Nat. Protoc.* **2008**, *3*, 163−175.
(23) Kumari, P.; Nath, Y.; Murty, U. S.; Ravichandiran, V.; Mohan, U. Sortase A Mediated Bioconjugation of Common Epitopes Decreases Biofilm Formation in Staphylococcus Aureus. *Front. Microbiol.* **2020**, *11*, 1702.
(24) Wallock-Richards, D. J.; Marles-Wright, J.; Clarke, D. J.; Maitra, A.; Dodds, M.; Hanley, B.; Campopiano, D. J. Molecular Basis of Streptococcus Mutans Sortase A Inhibition by the Flavonoid Natural Product Trans-Chalcone. *Chem. Commun.* **2015**, *51*, 10483−10485.
(25) Kim, S.; Chen, J.; Cheng, T.; Gindulyte, A.; He, J.; He, S.; Li, Q.; Shoemaker, B. A.; Thiessen, P. A.; Yu, B.; Zaslavsky, L.; Zhang, J.; Bolton, E. E. PubChem in 2021: New Data Content and Improved Web Interfaces. *Nucleic Acids Res.* **2021**, *49*, D1388−D1395.
(26) Daina, A.; Michielin, O.; Zoete, V. SwissADME: A Free Web Tool to Evaluate Pharmacokinetics, Drug-Likeness and Medicinal Chemistry Friendliness of Small Molecules. *Sci. Rep.* **2017**, *7*, 42717.
(27) Pires, D. E. v.; Blundell, T. L.; Ascher, D. B. PkCSM: Predicting Small-Molecule Pharmacokinetic and Toxicity Properties Using Graph-Based Signatures. *J. Med. Chem.* **2015**, *58*, 4066−4072.
(28) Yu, Z.; Han, J.; Liu, Y.; Zhu, J.; Tian, X.; Han, W. Molecular Dynamics Simulations and Steered Molecular Dynamics Simulations of Glabridin Bound to Wild Type and V30A Mutant Transthyretin: Ligand-Linked Perturbation of Tertiary Conformation. *Chem. Res. Chin. Univ.* **2018**, *34*, 995−1003.
(29) Trabalzini, L.; Ercoli, J.; Trezza, A.; Schiavo, I.; Macrì, G.; Moglia, A.; Spiga, O.; Finetti, F. Pharmacological and In Silico Analysis of Oat Avenanthramides as EGFR Inhibitors: Effects on EGF-Induced Lung Cancer Cell Growth and Migration. *Int. J. Mol. Sci.* **2022**, *23*, 8534.
(30) Kumar, N.; Garg, P. Probing the Molecular Basis of Cofactor Affinity and Conformational Dynamics of Mycobacterium Tuberculosis Elongation Factor Tu: An Integrated Approach Employing Steered Molecular Dynamics and Umbrella Sampling Simulations. *J. Phys. Chem. B* **2022**, *126*, 1447−1461.
(31) Kumar, S.; Bhardwaj, V. K.; Singh, R.; Das, P.; Purohit, R. Identification of Acridinedione Scaffolds as Potential Inhibitor of DENV-2 C Protein: An in Silico Strategy to Combat Dengue. *J. Cell. Biochem.* **2022**, *123*, 935−946.
(32) Parihar, A.; Ahmed, S. S.; Sharma, P.; Choudhary, N. K.; Akter, F.; Ali, M. A.; Sonia, Z. F.; Khan, R. Plant-Based Bioactive Molecules for Targeting of Endoribonuclease Using Steered Molecular Dynamic Simulation Approach: A Highly Conserved Therapeutic Target against Variants of SARS-CoV-2. *Mol. Simul.* **2022**, *49*, 1267−1279.
(33) Wang, A.; Yue, K.; Zhong, W.; Zhang, G.; Wang, L.; Wang, H.; Zhang, H.; Zhang, X. Ligand-Receptor Interaction in the Specific Targeting of Biomimetic Peptide Nanoparticles to Lysophosphatidylcholine. *Int. J. Biol. Macromol.* **2023**, *227*, 193−202.
(34) Reed, P.; Atilano, M. L.; Alves, R.; Hoiczyk, E.; Sher, X.; Reichmann, N. T.; Pereira, P. M.; Roemer, T.; Filipe, S. R.; Pereira-Leal, J. B.; Ligoxygakis, P.; Pinho, M. G. Staphylococcus Aureus Survives with a Minimal Peptidoglycan Synthesis Machine but Sacrifices Virulence and Antibiotic Resistance. *PLoS Pathog.* **2015**, *11*, No. e1004891.
(35) Foster, T. J. Antibiotic Resistance in Staphylococcus Aureus. Current Status and Future Prospects. *FEMS Microbiol. Rev.* **2017**, *41*, 430−449.
(36) Ma, Q.; Wang, G.; Li, N.; Wang, X.; Kang, X.; Mao, Y.; Wang, G. Insights into the Effects and Mechanism of Andrographolide-Mediated Recovery of Susceptibility of Methicillin-Resistant Staphylococcus Aureus to β-Lactam Antibiotics. *Microbiol. Spectr.* **2023**, *11*, 11.
(37) Warawa, J. M.; Duan, X.; Anderson, C. D.; Sotsky, J. B.; Cramer, D. E.; Pfeffer, T. L.; Guo, H.; Adcock, S.; Lepak, A. J.; Andes, D. R.; Slone, S. A.; Stromberg, A. J.; Gabbard, J. D.; Severson, W. E.; Lawrenz, M. B. Validated Preclinical Mouse Model for Therapeutic Testing against Multidrug-Resistant Pseudomonas Aeruginosa Strains. *Microbiol. Spectr.* **2022**, *10*, No. e02693.
(38) Jambrina, A. M.; Santomà, À.; Rocher, A.; Rams, N.; Cereza, G.; Rius, P.; Gironès, M.; Pareja, C.; Franch, À.; Rabanal, M. Detection and Prevention of Medication Errors by the Network of Sentinel Pharmacies in a Southern European Region. *J. Clin. Med.* **2022**, *12*, 194.
(39) Gaberino, C. L.; Chiu, A. M.; Mahatme, S. S. The Effects of Beta-Lactam Allergy Relabeling on Antibiotic Prescribing Practices. *Ann. Allergy Asthma Immunol.* **2022**, *128*, 307−313.
(40) Li, L.; Yin, Y.; Zheng, G.; Liu, S.; Zhao, C.; Ma, L.; Shan, Q.; Dai, X.; Wei, L.; Lin, J.; Xie, W. Determining β-Lactam Antibiotics in Aquaculture Products by Modified QuECHERS Combined with Ultra-High Performance Liquid Chromatography-Tandem Mass Spectrometry (UHPLC-MS/MS). *Arab. J. Chem.* **2022**, *15*, 103912.
(41) Le, P.; Kunold, E.; Macsics, R.; Rox, K.; Jennings, M. C.; Ugur, I.; Reinecke, M.; Chaves-Moreno, D.; Hackl, M. W.; Fetzer, C.; Mandl, F. A. M.; Lehmann, J.; Korotkov, V. S.; Hacker, S. M.; Kuster, B.; Antes, I.; Pieper, D. H.; Rohde, M.; Wuest, W. M.; Medina, E.; Sieber, S. A. Repurposing Human Kinase Inhibitors to Create an Antibiotic Active against Drug-Resistant Staphylococcus Aureus, Persisters and Biofilms. *Nat. Chem.* **2020**, *12*, 145−158.
(42) Kamurai, B.; Mombeshora, M.; Mukanganyama, S.; Khamesipour, F. Repurposing of Drugs for Antibacterial Activities on Selected ESKAPE Bacteria Staphylococcus Aureus and Pseudomonas Aeruginosa. *Int. J. Microbiol.* **2020**, *2020*, 1−9.
(43) Mahey, N.; Tambat, R.; Chandal, N.; Verma, D. K.; Thakur, K. G.; Nandanwar, H. Repurposing Approved Drugs as Fluoroquinolone Potentiators to Overcome Efflux Pump Resistance in Staphylococcus Aureus. *Microbiol. Spectr.* **2021**, *9*, No. e00951.
(44) Liu, Y.; Shi, Y.; Cheng, H.; Chen, J.; Wang, Z.; Meng, Q.; Tang, Y.; Yu, Z.; Zheng, J.; Shang, Y. Lapatinib Acts against Biofilm Formation and the Hemolytic Activity of Staphylococcus Aureus. *ACS Omega* **2022**, *7*, 9004−9014.
(45) Tang, Y.; Zou, F.; Chen, C.; Zhang, Y.; Shen, Z.; Liu, Y.; Deng, Q.; Yu, Z.; Wen, Z. Antibacterial and Antibiofilm Activities of Sertindole and Its Antibacterial Mechanism against Staphylococcus Aureus. *ACS Omega* **2023**, *8*, 5415−5425.
(46) Behmard, E.; Barzegari, E.; Najafipour, S.; Kouhpayeh, A.; Ghasemi, Y.; Asadi-Pooya, A. A. Efflux Dynamics of the Antiseizure Drug, Levetiracetam, through the P-Glycoprotein Channel Revealed by Advanced Comparative Molecular Simulations. *Sci. Rep.* **2022**, *12*, 13674.
(47) Kari, S.; Murugesan, A.; Thiyagarajan, R.; Kidambi, S.; Razzokov, J.; Selvaraj, C.; Kandhavelu, M.; Marimuthu, P. Bias-Force Guided Simulations Combined with Experimental Validations towards GPR17 Modulators Identification. *Biomed. Pharmacother.* **2023**, *160*, 114320.
(48) Xu, X.; Xu, L.; Yuan, G.; Wang, Y.; Qu, Y.; Zhou, M. Synergistic Combination of Two Antimicrobial Agents Closing Each

https://doi.org/10.1021/acsomega.3c02691
ACS Omega 2023, 8, 29292−29301

Other's Mutant Selection Windows to Prevent Antimicrobial Resistance. *Sci. Rep.* **2018**, *8*, 7237.
(49) Lázár, V.; Snitser, O.; Barkan, D.; Kishony, R. Antibiotic Combinations Reduce Staphylococcus Aureus Clearance. *Nature* **2022**, *610*, 540−546.
(50) Zhao, C.; Wistrand-Yuen, P.; Lagerbäck, P.; Tängdén, T.; Nielsen, E. I.; Friberg, L. E. Combination of Polymyxin B and Minocycline against Multidrug-Resistant Klebsiella Pneumoniae: Interaction Quantified by Pharmacokinetic/Pharmacodynamic Modelling from in Vitro Data. *Int. J. Antimicrob. Agents* **2020**, *55*, 105941.
(51) Lin, F.; Yu, B.; Wang, Q.; Yuan, M.; Ling, B. Combination Inhibition Activity of Chlorhexidine and Antibiotics on Multidrug-Resistant Acinetobacter Baumannii in Vitro. *BMC Infect. Dis.* **2021**, *21*, 266.
(52) Sun, D.; Gao, W.; Hu, H.; Zhou, S. Why 90% of Clinical Drug Development Fails and How to Improve It? *Acta Pharm. Sin. B* **2022**, *12*, 3049−3062.
(53) Danielson, M. L.; Hu, B.; Shen, J.; Desai, P. v. In Silico ADME Techniques Used in Early-Phase Drug Discovery; **2017**; pp 81−117. https://doi.org/ DOI: 10.1007/978-3-319-50042-3_4.
(54) Daina, A.; Zoete, V. A BOILED-Egg To Predict Gastrointestinal Absorption and Brain Penetration of Small Molecules. *ChemMedChem* **2016**, *11*, 1117−1121.
(55) Hollenberg, P. F. Characteristics and Common Properties of Inhibitors, Inducers, and Activators of CYP Enzymes. *Drug Metab. Rev.* **2002**, *34*, 17−35.
(56) Huang, S.-M.; Strong, J. M.; Zhang, L.; Reynolds, K. S.; Nallani, S.; Temple, R.; Abraham, S.; Habet, S.; Baweja, R. K.; Burckart, G. J.; Chung, S.; Colangelo, P.; Frucht, D.; Green, M. D.; Hepp, P.; Karnaukhova, E.; Ko, H.-S.; Lee, J.-I.; Marroum, P. J.; Norden, J. M.; Qiu, W.; Rahman, A.; Sobel, S.; Stifano, T.; Thummel, K.; Wei, X.-X.; Yasuda, S.; Zheng, J. H.; Zhao, H.; Lesko, L. J. New Era in Drug Interaction Evaluation: US Food and Drug Administration Update on CYP Enzymes, Transporters, and the Guidance Process. *J. Clin. Pharmacol.* **2008**, *48*, 662−670.
(57) Kirchmair, J.; Göller, A. H.; Lang, D.; Kunze, J.; Testa, B.; Wilson, I. D.; Glen, R. C.; Schneider, G. Predicting Drug Metabolism: Experiment and/or Computation? *Nat. Rev. Drug Discov.* **2015**, *14*, 387−404.

https://doi.org/10.1021/acsomega.3c02691
ACS Omega 2023, 8, 29292−29301